PRMT1 accelerates cell proliferation, migration, and tumor growth by upregulating ZEB1/H4R3me2as in thyroid carcinoma

GUOLI FENG[1], CHANGJU CHEN[2] and YI LUO[1]

[1]Department of General Surgery, Department of Thyroid and Breast Surgery; [2]Department of Medical, Affiliated Hospital of Zunyi Medical University, Zunyi, Guizhou 563000, P.R. China

Received March 20, 2023; Accepted September 21, 2023

DOI: 10.3892/or.2023.8647

Abstract. Thyroid carcinoma (TC) represents the most prevalent malignancy of the endocrine system. Protein arginine methyltransferase 1 (PRMT1) is a critical member of the protein arginine methyltransferase family in mammals and is involved in multiple biological processes. This study aimed to investigate the function of PRMT1 in TC. In the present study, human TC cell lines (8505C, CAL62, and BCPAP) and a normal human thyroid cell line Nthy-ori 3-1 were employed. Small interfering RNA targeting PRMT1 was used to knock down PRMT1 expression in 8505C cells, and PRMT1 overexpression plasmids were transfected into BCPAP cells. Cell viability was assessed using a CCK-8 and colony formation assays. Apoptosis was measured using flow cytometry and TUNEL assays. Cell migration was assessed using wound healing and Transwell assays. Reverse transcription-quantitative PCR was used to determine the mRNA expression levels of PRMT1. Western blotting was used to detect the protein expression levels of PRMT1, E-cadherin, vimentin, H4R3me2as, and zinc-finger E homeobox-binding 1 (ZEB1). Notably, PRMT1 expression was elevated in TC ($P<0.01$). PRMT1 knockdown inhibited TC cell proliferation and migration and concurrently enhanced migration. Furthermore, PRMT1 knockdown suppressed tumor growth and metastasis in a mouse model of TC. PRMT1 downregulation increased E-cadherin expression and decreased the expression of vimentin, H4R3me2as, and ZEB1 in the TC cells and the mouse model of TC. Conversely, PRMT1 overexpression had the opposite effect on TC malignant characteristics ($P<0.05$). These findings suggest that PRMT1 knockdown inhibited TC malignancy by downregulating H4R3me2as/ZEB1, thereby highlighting novel therapeutic targets and diagnostic markers for the management of TC.

Correspondence to: Dr Guoli Feng, Department of General Surgery, Department of Thyroid and Breast Surgery, Affiliated Hospital of Zunyi Medical University, 149 Dalian Road, Zunyi, Guizhou 563000, P.R. China
E-mail: fenggl@zmu.edu.cn

Abbreviations: TC, thyroid carcinoma; PRMT1, protein arginine methyltransferase 1; ZEB1, zinc-finger E homeobox-binding 1; EMT, epithelial-mesenchymal transition

Key words: thyroid carcinoma, protein arginine methyltransferase 1, H4R3me2, ZEB1, malignancy

Introduction

Thyroid carcinoma (TC) is the most prevalent malignant endocrine neoplasm originating from either the thyroid follicular or parafollicular epithelial cells (1). Notably, it constitutes ~12% of newly diagnosed cancers in adolescents and has witnessed a steady increase in incidence rates (2,3). Predominantly affecting females, TC ranks as the second most common cancer in young women aged 18-35 years old (4). Multiple carcinogenic factors, including nutrition/dietary practices, obesity, and radiation exposure, synergistically contribute to the onset of TC (5). Current therapeutic modalities, which include radiation, thyroid hormone therapy, and surgery, are frequently employed in combination (5,6). Although the treatment of TC is improving, owing to the lack of precise molecular targets, the overall 5-year survival rate of patients with TC remains suboptimal, particularly in patients with advanced clinical stage TC (7). Therefore, there is an urgent need to improve our understanding of the underlying mechanisms and to identify novel therapeutic strategies for the management of TC.

Arginine methyltransferase 1 (PRMT1), a member of the PRMT family, plays an important role in arginine methylation (8). PRMT1 can coactivate the histone code and epigenetic control by methylating histone H4 at the third arginine residue (H4R3) (9), in particular H4R3me2as, which is a marker of transcriptional activation (10). PRMT1 modulates epigenetic changes in physiological and pathophysiological processes including cell proliferation, survival, and metabolism (11). Increased PRMT1 expression drives tumorigenesis and progression in various types of cancer, including lung, breast, and prostate cancer (12-14). Collectively, these results indicate that PRMT1 contributes to cancer progression by methylating both histone and non-histone proteins. A previous study revealed that PRMT1 was aberrantly expressed in TC tumor tissues compared with normal tissues (15). However, to the best of the authors' knowledge, there are no studies assessing the function of PRMT1 in TC.

Zinc-finger E homeobox-binding 1 (ZEB1) is an important transcription factor for epithelial-mesenchymal transition (EMT) (16). It is aberrantly expressed in several types of cancer, including gastric, colorectal, and cervical cancer (17-19). Evidence has shown that PRMT1 modulates EMT by regulating ZEB1 expression in breast cancer (20). Furthermore, ZEB1 expression is associated with PRMT1 expression in pancreatic cancer cells (21). However, it remains unclear whether PRMT1 regulates ZEB1 expression in TC.

In this study, the effect of PRMT1 on TC cell proliferation, migration, and apoptosis was assessed by modulating its expression *in vitro* using TC cell lines and *in vivo* using a xenograft mouse model. This study offers a novel perspective for potential therapeutic avenues in the management of TC.

Materials and methods

Cell culture. Human TC cell lines (8505C, CAL62, and BCPAP) and the normal human thyroid cell line Nthy-ori 3-1 were supplied by the National Collection of Authenticated Cell Cultures. The BCPAP cells were authenticated using short tandem repeat profiling (iCell Bioscience, Inc.). 8505C and CAL62 cells were cultured in DMEM (Gibco; Thermo Fisher Scientific, Inc.), whereas BCPAP and Nthy-ori 3-1 cells were cultured in RPMI-1640 medium (Gibco; Thermo Fisher Scientific, Inc.). In both cases, media was supplemented with 10% FBS (MilliporeSigma) and cells were maintained in a humidified incubator supplied with 5% CO_2 air at 37˚C.

Cell transfection and treatment. PRMT1 small interfering RNA (siRNA; si-PRMT1), negative control (si-NC), si-ZEB1, and a PRMTI overexpression plasmid (oe-PRMT1) were designed by Tsingke Biotechnology Co., Ltd. The cells were cultured to 70-80% confluence in six-well plates. Next, 8505C cells were transfected with 50 nM si-PRMT1 or si-NC and BCPAP cells with 0.8 μg oe-PRMT1 or co-transfected with si-ZEB1 using the Lipofectamine® 3000 system (Invitrogen; Thermo Fisher Scientific, Inc.) for 6 h. The sequences of siRNA were: si-PRMT1, GCCTACTTCAACATCGAG T; si-ZEB1, TGCAGAAAATGAGCAAAACCATG; and si-NC, TTCTCCGAACGTGTCACG. Cells transfected with si-PRMT1 were then treated with 10 or 50 μM AMI-1 (a PRMT1 inhibitor; T2352; TargetMol) for 48 h, or otherwise untreated and used as control cells.

CCK-8 assay. Cell viability was determined using a CCK-8 assay kit (Beyotime Institute of Biotechnology), according to the manufacturer's instructions. The 8505C or BCPAP cells ($5x10^3$ cells/well) were placed into 96-well plates and cultured for 0, 10, or 24 h for 8505C cells, or 0, 48, and 72 h for BCPAP, after which they were treated with 10 μl CCK-8 reagent for a further 2 h. Subsequently, the absorbance at 450 nm was measured using a microplate reader (Thermo Fisher Scientific, Inc.).

Colony formation assay. BCPAP and 8505C cells ($1x10^3$ cells/well) were incubated for 7 days in six-well plates. The cells were fixed with 4% paraformaldehyde for 15 min and stained with 0.1% crystal violet (Sangon Biotech) for 10 min both at room temperature, after which cells were imaged using a light microscope at x100 magnification (Olympus Corporation). The number of colonies in five random, non-overlapping fields of view were counted and averaged.

Flow cytometry assay. Apoptosis was assessed using an Annexin V-FITC Apoptosis Detection Kit (MilliporeSigma). BCPCP and 8505C cells were seeded in six-well plates at a density of $1x10^5$ cells/well. Cells were allowed to adhere overnight after which the cells were stained with Annexin V/PI for 10 min at room temperature and the percentage of apoptotic cells was examined using a flow cytometer (FACSCalibur; BD Biosciences) and analyzed using CellQuest software 3.3 (BD Biosciences).

Wound healing assay. The cells were incubated until they were 90% confluent in six-well plates. The monolayer of cells was scratched using a 100 μl pipette tip. After removing the detached cells using PBS, the cells were imaged (0 h) and then incubated for 24 h and imaged again (24 h). Cell images were acquired using an inverted light microscope (Olympus Corporation) at 0 and 24 h. The wound width was measured using Image-Pro Plus 6.0 (Media Cybernetics, Inc.).

Transwell assays. Cell migration was determined using a Corning BioCoat Matrigel Invasion Chamber (Corning, NY, USA). To the upper chamber of the Transwell insert, a 200 μl of serum-free cell suspension ($5x10^4$ cells) was added. Medium (600 μl) with 10% FBS was added to the lower chambers. After 24 h of incubation, the invaded cells were fixed with 4% paraformaldehyde for 30 min and stained with crystal violet for an additional 30 min both at room temperature. Cells were counted in five arbitrary optical fields of view under a light microscope (magnification, x200; Olympus Corporation).

Reverse transcription-quantitative polymerase chain reaction (RT-qPCR). Total RNA was extracted from TC tissues and cells using the TRIzol® reagent (Invitrogen; Thermo Fisher Scientific, Inc.). cDNA was synthesized using the FastKing-RT SuperMix (Tiangen Biotech Co., Ltd.). Next, Super SYBR Green qPCR Master mix (Life Inc.) was used for PCR amplification using a real-time PCR system (Bio-Rad Laboratories, Inc.). The amplification conditions were 95˚C for 3 min for denaturation; followed by 40 cycles of 95˚C for 5 sec, and 60˚C for 45 sec. Relative mRNA expression was determined using the $2^{-\Delta\Delta Cq}$ method (22), with β-actin serving as an internal control. The primer sequences used were: PRMT1 forward, 5'-ACTGCCTCTTCTACGAGTCCA-3' and reverse, 5'-TGCACGTAGTCATTCCGCTT-3'; ZEB1 forward, 5'-ACT CTGATTCTACACCGC-3' and reverse, 5'-TGTCACATTGAT AGGGCTT-3'; and β-actin forward, 5'-GACAGGATGCAG AAGGAGATTACT-3' and reverse, 5'-TGATCCACATCT GCTGGAAGGT-3'.

Xenograft mouse model. All animal experiments were approved by the Institutional Animal Care and Use Committee of the Affiliated Hospital of the Zunyi Medical University (approval no. zyfy-an-2023-0185). BALB/C nude mice (female, 6 weeks, 18-20 g, n=16) were supplied by GemPharmatech and fed in specific pathogen-free facilities with a 12/12 h light/dark cycle at 22-24˚C. All the

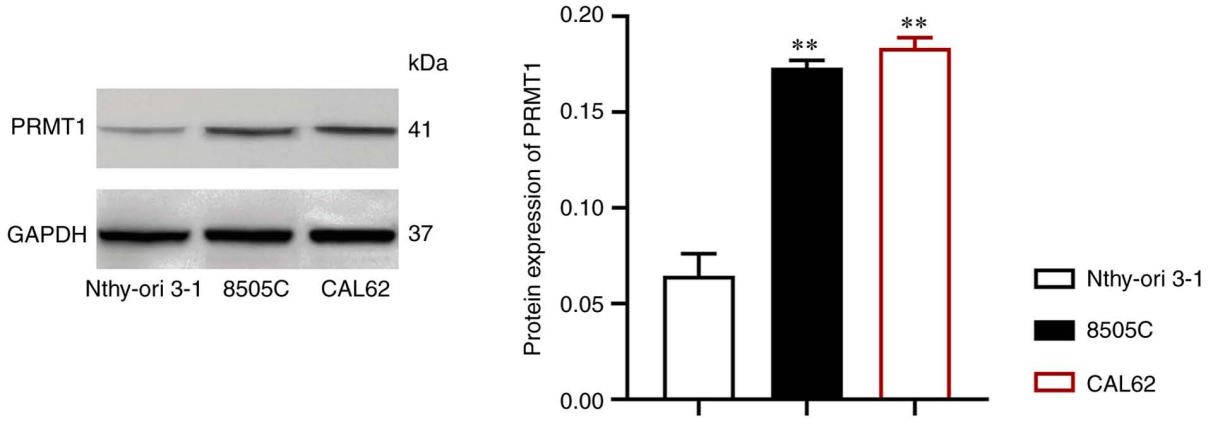

Figure 1. PRMT1 expression is upregulated in TC cells. Western blotting was used to detect the expression of PRMT1 in human TC cell lines 8505C and CAL62, and in the human normal thyroid cell line Nthy-ori 3-1. **P<0.01 vs. Nthy-ori 3-1. PRMT1, protein arginine methyltransferase 1; TC, thyroid carcinoma.

mice had *ad libitum* access to food and water during the experimental period. To establish TC tumor-bearing mice, 8505C or PRMT1-knockdown 8505C cell suspensions ($4x10^6$ cells/mouse) were subcutaneously injected every 4 days (n=4 in each group). Tumor volume was monitored every 3 days and calculated as volume=0.5 x length x $width^2$. To assess TC pulmonary metastasis in a nude mouse model, cell suspensions ($1x10^6$) were injected into mice through the tail vein. After 28 days, the mice anesthetized using 2% pentobarbital sodium (30 mg/kg), followed by euthanasia by cervical dislocation. The tumors were harvested, weighed, images captured with a camera (Leica Camera AG), and prepared for subsequent examination.

Hematoxylin and eosin (H&E) staining. Thyroid tumor tissues were fixed in 10% neutral-buffered formalin. Paraffin-embedded tissues were then cut into 4 μm-thick sections and stained using hematoxylin for 5 min and eosin for 2 min at room temperature after dewaxing. Finally, histological changes in the tumor sections were analyzed under a light microscope (Olympus Corporation).

TUNEL analysis. Cytospin preparations of tumor sections were examined using a TUNEL assay. Samples were permeabilized with 0.1% Triton X-100 in 0.1% sodium citrate for 2 min on ice and fixed for 15 min with 4% paraformaldehyde. The TUNEL assay was performed using an *in-situ* cell death detection kit according to the manufacturer's protocol (Fluorescein; Roche Diagnostics GmbH).

Immunofluorescence (IF) analysis. Cells were resuspended in media supplemented with 10% FBS and cultured for 6 h on chamber slides, after which they were fixed in ice-cold 80% methanol for 10 min. Permeabilization was performed using 0.5% Triton X-100 (MilliporeSigma) for 10 min. The cells were then incubated with anti-vimentin (cat. no. ab286811, 1:100; Abcam) or anti-E-cadherin (cat. no. ab40772, 1:500; Abcam) fluorescent primary antibodies for 60 min at room temperature. Then, samples were counterstained with 1 μg/ml DAPI for 5 min at room temperature, and slides were imaged using a fluorescence microscope (magnification, x400; Olympus Corporation).

Western blotting. Total protein was acquired from TC tumor tissues and cells using RIPA lysis buffer (Beyotime Institute of Biotechnology) and protein concentration was measured using a BCA kit (Beyotime Institute of Biotechnology). A total of 20 μg protein was loaded on a 10% SDS gel, resolved using SDS-PAGE, and transferred to a PVDF membrane (Beyotime Institute of Biotechnology). After blocking with 5% non-fat milk, the membrane was incubated overnight at 4˚C with one of the following primary antibodies: Anti-PRMT1 (cat. no. ab73246; 1:500; Abcam), anti-E-cadherin (cat. no. ab40772; 1:10,000; Abcam), anti-vimentin (cat. no. ab137321; 1:1,000; Abcam), anti-ZEB1 (cat. no. ab81972; 1:2,000; Abcam), anti-H4R3me2as (cat. no. 39705; 1:1,000; Active Motif), or anti-GAPDH (cat. no. ab9485; 1:2,500; Abcam). The membrane was then incubated with a goat anti-rabbit IgG secondary antibody (cat. no. ab205718; 1:2,000; Abcam) for 60 min. Protein bands were observed using ECL reagent (Wuhan Servicebio Technology Co., Ltd.) and quantified using ImageJ version 1.8.0 (National Institutes of Health).

Statistical analysis. Data are presented as the mean ± SD of at least 3 independent repeats. Differences between ≥3 groups were compared using a one-way ANOVA followed by a post hoc Tukey's test. Differences between 2 groups were compared using a Student's t-test. GraphPad Prism version 8.0 (GraphPad Software, Inc.) was used for statistical analyses. P<0.05 was considered to indicate a statistically significant difference.

Results

PRMT1 is upregulated in TC. First, PRMT1 expression in the TC cell lines 8505C and CAL62 was assessed and compared with that in Nthy-ori 3-1 cells. Notably, PRMT1 expression was significantly upregulated in the TC cell lines (P<0.01; Fig. 1).

PRMT1 knockdown inhibits cell proliferation and migration and promotes cell apoptosis in TC. 8505C cells are a mesenchymal TC cell line, and it has been shown that the upregulated genes in the mesenchymal TC cell line are primarily involved in DNA replication and exhibit increased

proliferative and migratory capacity compared with other cell lines (23). Therefore, si-PRMT1 was transfected into 8505C cells, and cells treated with PRMT1 inhibitor (10 or 50 μM AMI-1) were used as positive controls. The results showed that the expression of PRMT1 mRNA and protein was reduced in 8505C cells after treatment with AMI-1 or transfected with si-PRMT1 (P<0.01; Fig. 2A and B). si-PRMT1 transfection exhibited a better ability in reducing PRMT1 expression than did treatment with AMI-1 (P<0.01; Fig. 2A and B). The CCK-8 assays showed a marked decrease in cell viability following PRMT1 knockdown (P<0.01; Fig. 2C). Additionally, the colony formation rate decreased upon PRMT1 knockdown (P<0.01; Fig. 2D). Apoptosis was increased following knockdown of PRMT1 (P<0.01; Fig. 2E). Wound healing and Transwell assays were used to further verify the effect of PRMT1 knockdown on cell migration (P<0.01; Fig. 2F and G). The levels of PRMT1 expression and cell proliferation, colony formation, and migration of 8505C cells treated with 50 μM AMI-1 were significantly lower than those of cells treated with 10 μM AMI-1 (P0.05; Fig. 2A-G). These results demonstrated that PRMT1 knockdown/inhibition reduced the metastatic potential and increased the apoptosis of TC cells.

PRMT1 knockdown suppresses cell metastasis and downregulates the expression of ZEB1 and H4R3me2as in TC. Subsequently, the inhibitory mechanism of PRMT1 knockdown on TC progression was assessed by determining the expression of E-cadherin, vimentin, ZEB1, and H4R3me2as in 8505C cells treated with or without si-PRMT1 or AMI-1. IF results indicated that E-cadherin expression increased, whereas vimentin expression decreased in 8505C cells treated with AMI-1 or si-PRMT1 compared to si-NC cells (Fig. 3A). Western blotting was used to further verify that PRMT1 downregulation promoted E-cadherin expression (P<0.01) and reduced vimentin expression (P<0.01; Fig. 3B). AMI-1 exerted its effect on the levels of E-cadherin and vimentin in a dose-dependent manner, and 50 μM AMI-1 showed a better efficiency in regulating the expression of E-cadherin and vimentin than si-PRMT1 (P<0.01; Fig. 3B).

PRMT1 downregulation also decreased the protein expression levels of ZEB1 and H4R3me2as (P<0.01; Fig. 3B). Notably, si-PRMT1 exhibited a better effect on reversing ZEB1 expression compared with 10 μM AMI-1 (P<0.01; Fig. 3B).

PRMT1 overexpression accelerates TC progression by downregulating the expression of ZEB1 and H4R3me2as. To further verify the role of PRMT1 on the malignant characteristics of TC, PRMT1 was overexpressed in BCPAP cells, a TC cell line that has been previously used as a control of 8505C cells (24). PRMT1 expression was successfully upregulated after transfection with oe-PRMT1 (P<0.01; Fig. 4A and B). Compared with the control cells, PRMT1 overexpression promoted cell proliferation and migration (P<0.05) but did not significantly affect apoptosis (P=0.06; Fig. 4C-G). Additionally, E-cadherin expression was downregulated, and vimentin expression was upregulated in BCPAP cells upon PRMT1 overexpression (P<0.05; Fig. 4H and I). PRMT1 overexpression increased the expression of ZEB1 and H4R3me2as in BCPAP cells (P<0.01; Fig. 4I). This study further demonstrates that PRMT1 promotes TC progression by upregulating the expression of ZEB1 and H4R3me2as.

Subsequently, BCPAP cells were co-transfected with oe-PRMT1 and si-ZEB1. As shown in Fig. 5A and B, ZEB1 expression was successfully knocked down following si-ZEB1 transfection, and PRMT1 expression was elevated in BCPAP cells (P<0.01). ZEB1 knockdown reversed the effects of PRMT1 overexpression on promoting cell proliferation, migration, and expression of vimentin and E-cadherin (P<0.01; Fig. 5C-G). Additionally, ZEB1 inhibition downregulated the protein expression of H4R3me2as induced by oe-PRMT1 (P<0.01; Fig. 5G).

PRMT1 knockdown reduces tumor growth and metastasis by downregulating ZEB1/H4R3me2as in a xenograft mouse model of TC. A TC xenograft mouse model was established to explore the effects of PRMT1 on tumor growth. PRMT1 protein levels were reduced in TC tumor tissues from tumor-bearing mice treated with si-PRMT1 or AMI-1 compared with those in the control group (P<0.01; Fig. 6A). The data showed that PRMT1 downregulation inhibited tumor growth in mice (P<0.01; Fig. 6B). Cells in the si-NC group exhibited apparent ablation, and the nuclei showed nuclear pleomorphism and small nucleoli; however, PRMT1 downregulation ameliorated these phenomena (Fig. 6C). Moreover, there were pulmonary nodules in the lungs of mice with TC, and the extent of these nodules was reduced in the mice injected with the PRMT1 knockdown cells (P<0.01; Fig. 6D). TUNEL apoptosis assays showed that the number of positive cells increased following PRMT1 knockdown (Fig. 6E). Western blotting indicated that E-cadherin expression was upregulated, whereas the expression of vimentin, ZEB1, and H4R3me2as was decreased following PRMT1 knockdown (P<0.05; Fig. 6F). Additionally, AMI-1 regulated tumor growth and the expression these proteins in a dose-dependent manner, and 50 μM AMI-1 exhibited a more potent effect than si-PRMT1 (P<0.05; Fig. 6A-F).

Discussion

TC is the most prevalent endocrine neoplasm (1). PRMT1, which catalyzes the protein methylation of arginine residues, plays a crucial role in tumorigenesis (25). In the present study, PRMT1 expression was increased in TC, and its downregulation inhibited cell proliferation and migration, as well as tumor growth and metastasis. Furthermore, the expression levels of ZEB1 and H4R3me2as were determined to be associated with those of PRMT1, suggesting a novel PRMT1/ZEB1/H4R3me2as axis that is involved in the malignant progression of TC.

PRMT1 is the primary type I PRMT, and accounts for 85% of the activity of type I PRMTs in mammals. PRMT1 participates in various cellular processes due to the diversity of its histone and non-histone substrates (26). Previous studies have implicated PRMT1 in various cancers, as it regulates post-translational modifications that are crucial for cancer pathophysiology (27,28). PRMT1 expression can be used to predict the outcomes of neoadjuvant treatments for locally advanced uterine cervical cancer (29). Li *et al* (30) reported that PRMT1 promoted breast cancer cell proliferation and tumorigenesis. In the present study, PRMT1 upregulation was

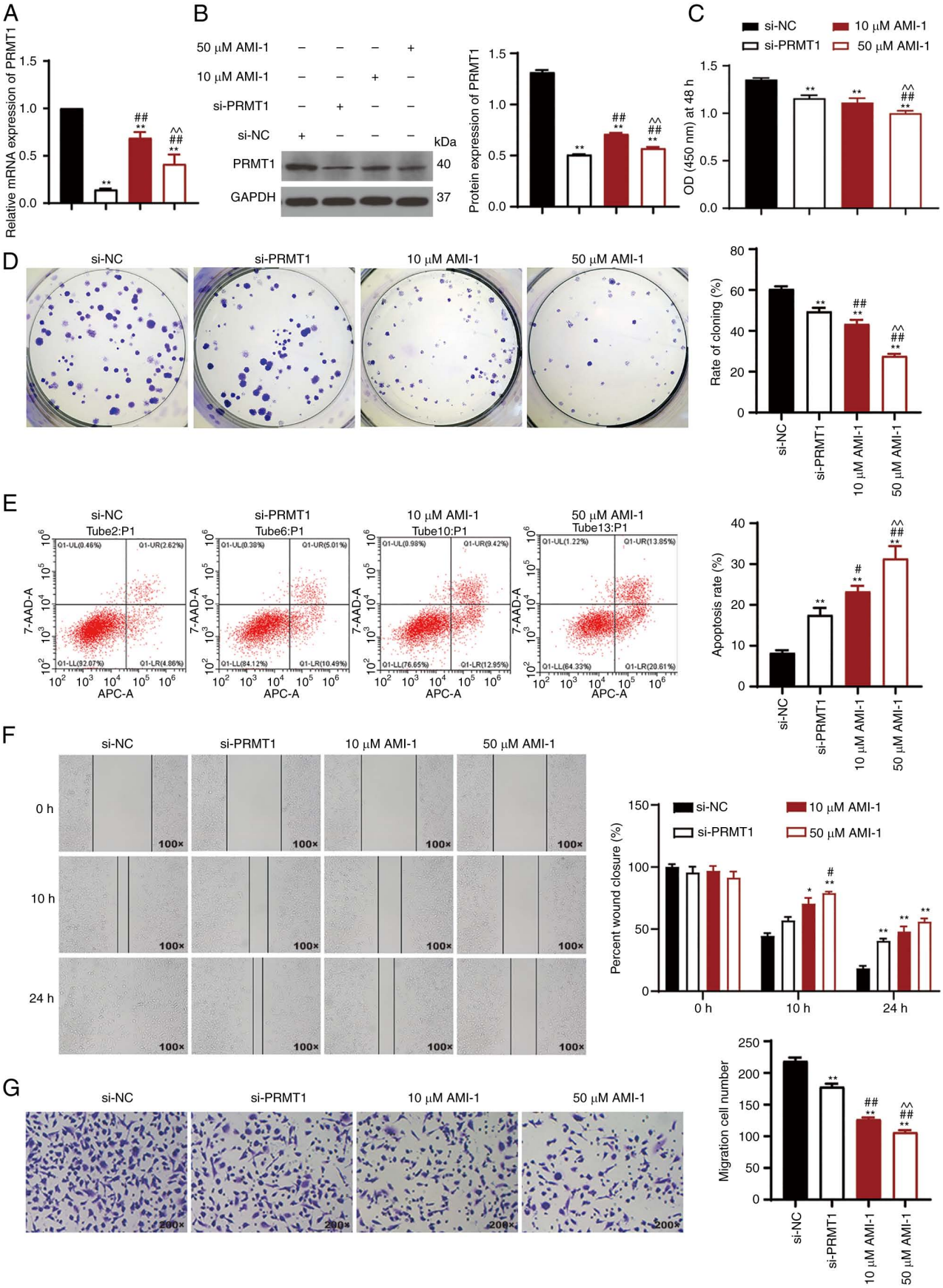

Figure 2. PRMT1 downregulation inhibits cell proliferation and migration and promotes cell apoptosis in TC. (A and B) RT-qPCR and western bolting were used to determine the expression of PRMT1 in 8505C cells following various treatments. (C and D) CCK-8 and colony formation assays were used to assess cell viability and proliferation, respectively, of treated 8050C cells. (E) Flow cytometry was used to determine apoptosis of treated 8505C cells. (F and G) Wound healing (magnification, x100) and Transwell (magnification, x200) assays were used to assess cell migration of the treated 8505C cells. *P<0.05, **P<0.01 vs. si-NC; $^{\#}$P<0.05, $^{\#\#}$P<0.01 vs. si-PRMT1; $^{\wedge\wedge}$P<0.01 vs. 10 μM AMI-1. PRMT1, protein arginine methyltransferase 1; TC, thyroid carcinoma; si-NC, small interfering RNA negative control.

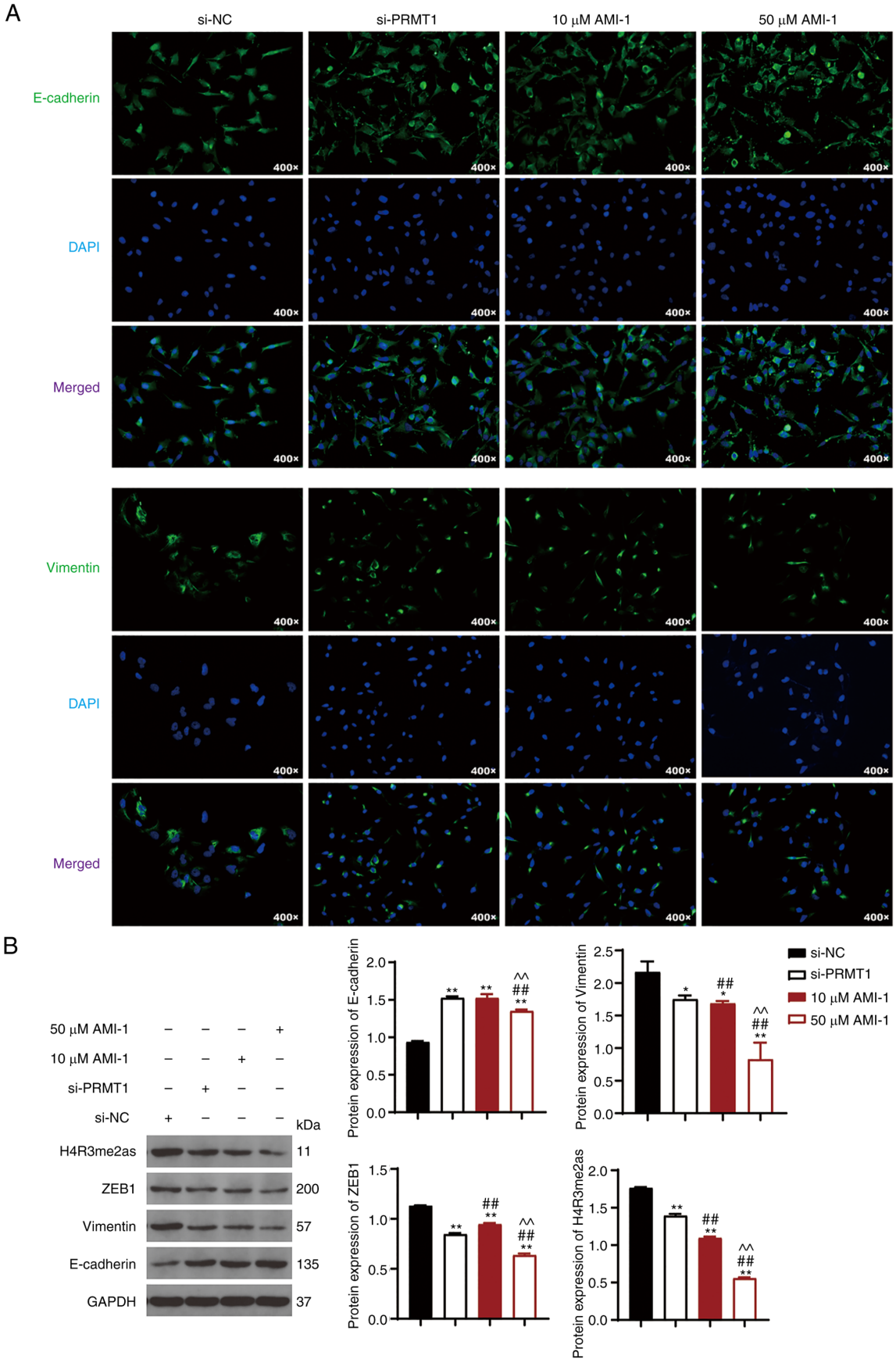

Figure 3. PRMT1 knockdown suppresses cell metastasis and downregulates expression of ZEB1 and H4R3me2as in TC. (A) IF analyzed the contents of E-cadherin and vimentin in 8505C cells, magnification=400x. (B) Western blotting was used to assess the protein expression levels of E-cadherin, vimentin, H4R3me2as, and ZEB1 in 8505C cells. The 8505C cells were transfected with si-NC or si-PRMT1. *P<0.05, **P<0.01 compared with si-NC; $^{\#\#}$P<0.01 compared with si-PRMT1; $^{\wedge\wedge}$P<0.01 compared with 10 μM AMI-1. Each experiment was conducted at least thrice. PRMT1, protein arginine methyltransferase 1; ZEB1, zinc finger e-box binding homeobox1, H4R3me2as, asymmetric demethylation of H4 at the third arginine residue; TC, thyroid carcinoma; si-NC, small interfering RNA negative control.

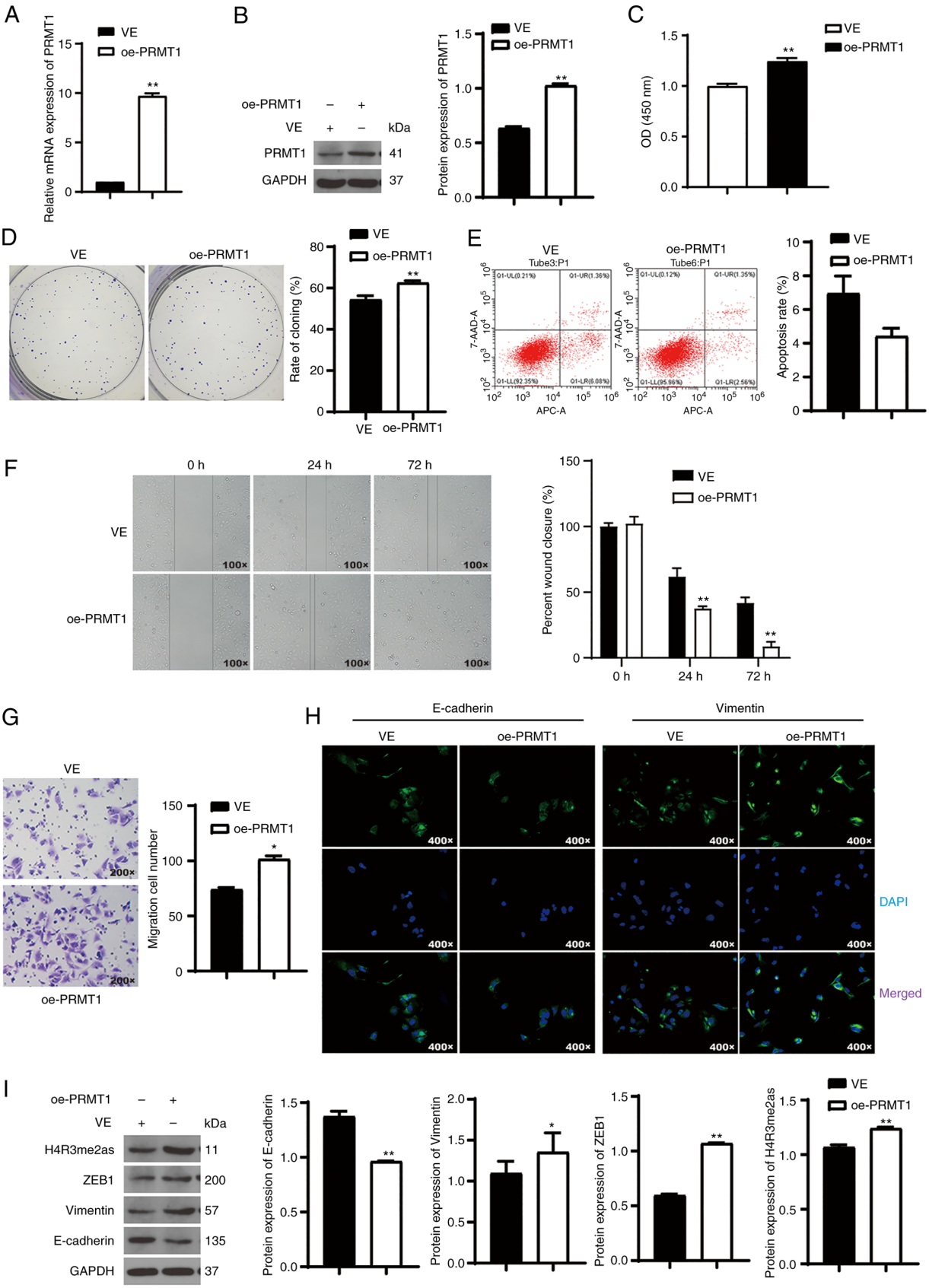

Figure 4. PRMT1 overexpression accelerates TC progression and upregulates the expression of ZEB1 and H4R3me2as. (A and B) RT-qPCR and western bolting were used to assess the expression of PRMT1 in BCPAP cells. (C and D) The CCK-8 and colony formation analyses were used to determine BCPAP cell viability and proliferation, respectively. (E) Flow cytometry was used to analyze BCPAP cell apoptosis. (F and G) Wound healing (magnification, x100) and Transwell (magnification, x200) assays were used to assess cell migration of BCPAP cells. (H) IF was used to assess E-cadherin and vimentin expression in BCPAP cells. Magnification, x400. (I) Western blotting was used to assess the protein expression of E-cadherin, vimentin, H4R3me2as, and ZEB1 in BCPAP cells. BCPAP cells were transfected with oe-PRMT1. *P<0.05, **P<0.01 vs. with VE. PRMT1, protein arginine methyltransferase 1; ZEB1, zinc finger e-box binding homeobox1; H4R3me2as, asymmetric demethylation of H4 at the third arginine residue; TC, thyroid carcinoma; oe-PRMT1, overexpression-PRMT1; VE, vector.

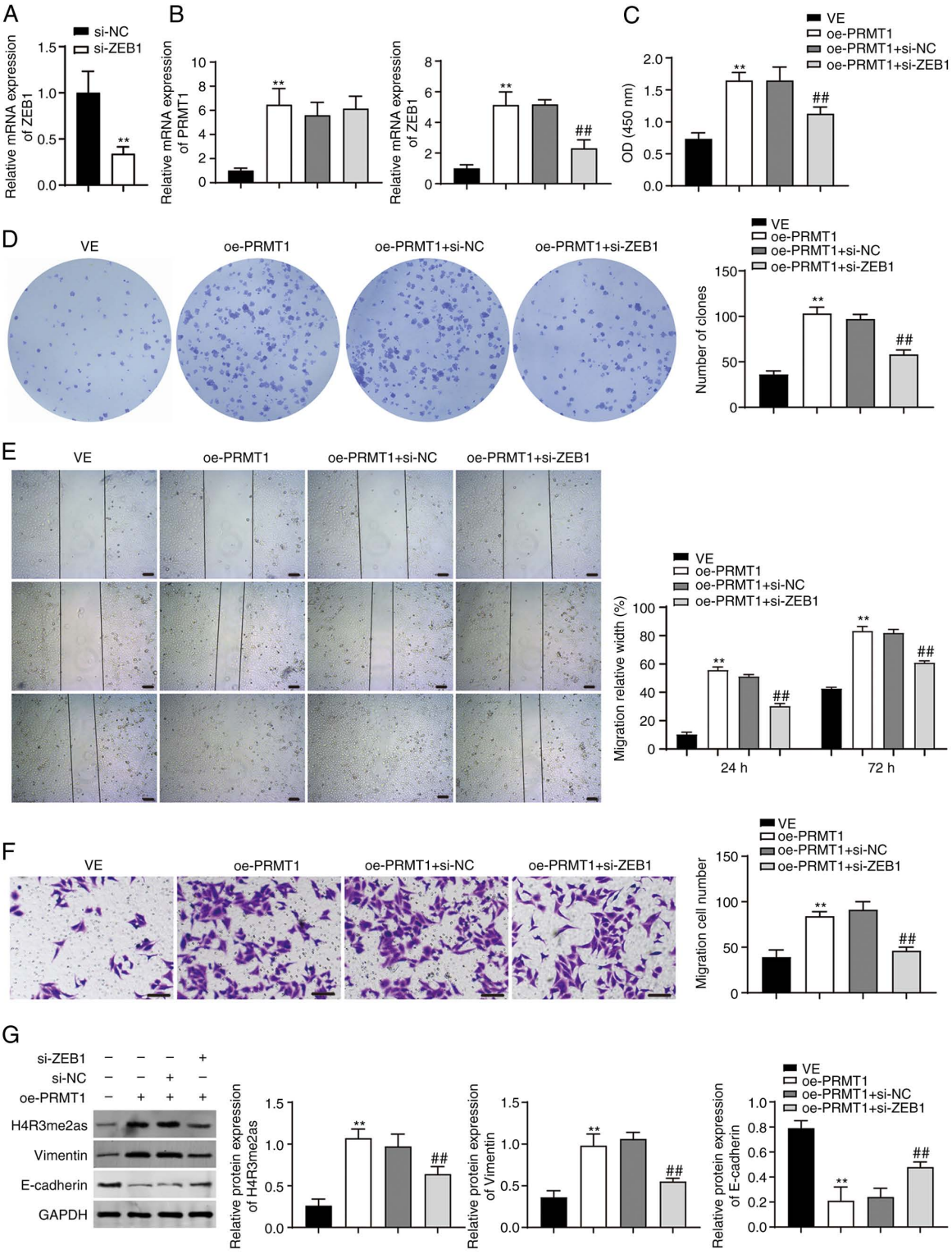

Figure 5. PRMT1 overexpression accelerates TC progression through the activation of ZEB1/H4R3me2as. (A) RT-qPCR was used to assess the expression of ZEB1 in BCPAP cells transfected with si-ZEB1. (B) mRNA expression of PRMT1 and ZEB1 in multiple group of cells. (C and D) CCK-8 and colony formation assays were used to test BCPAP cell viability and proliferation, respectively. (E and F) Wound healing and Transwell assays were used to assess cell migration of BCPAP cells. Scale bar, 50 μM. (G) Western blotting was used to measure the protein expression levels of E-cadherin, vimentin, and H4R3me2as in BCPAP cells. BCPAP cells were transfected with oe-PRMT1 and/or si-ZEB1. **P<0.01 vs. VE group, $^{\#\#}$P<0.01 vs. oe-PRMT1 + si-NC group. PRMT1, protein arginine methyltransferase 1; ZEB1, zinc finger e-box binding homeobox1; H4R3me2as, asymmetric demethylation of H4 at the third arginine residue; TC, thyroid carcinoma; oe-PRMT1, overexpression-PRMT1; VE, vector.

observed in a TC cell line. Subsequent experiments revealed that PRMT1 knockdown suppressed TC cell proliferation and migration, whereas its overexpression accelerated these processes. In addition, PRMT1 delayed TC tumor growth and metastasis in a xenograft tumor mouse model. These results indicated that PRMT1 was associated with TC tumorigenesis.

EMT is a morphogenetic reversible process related to tumor initiation, invasion, metastasis, and resistance to

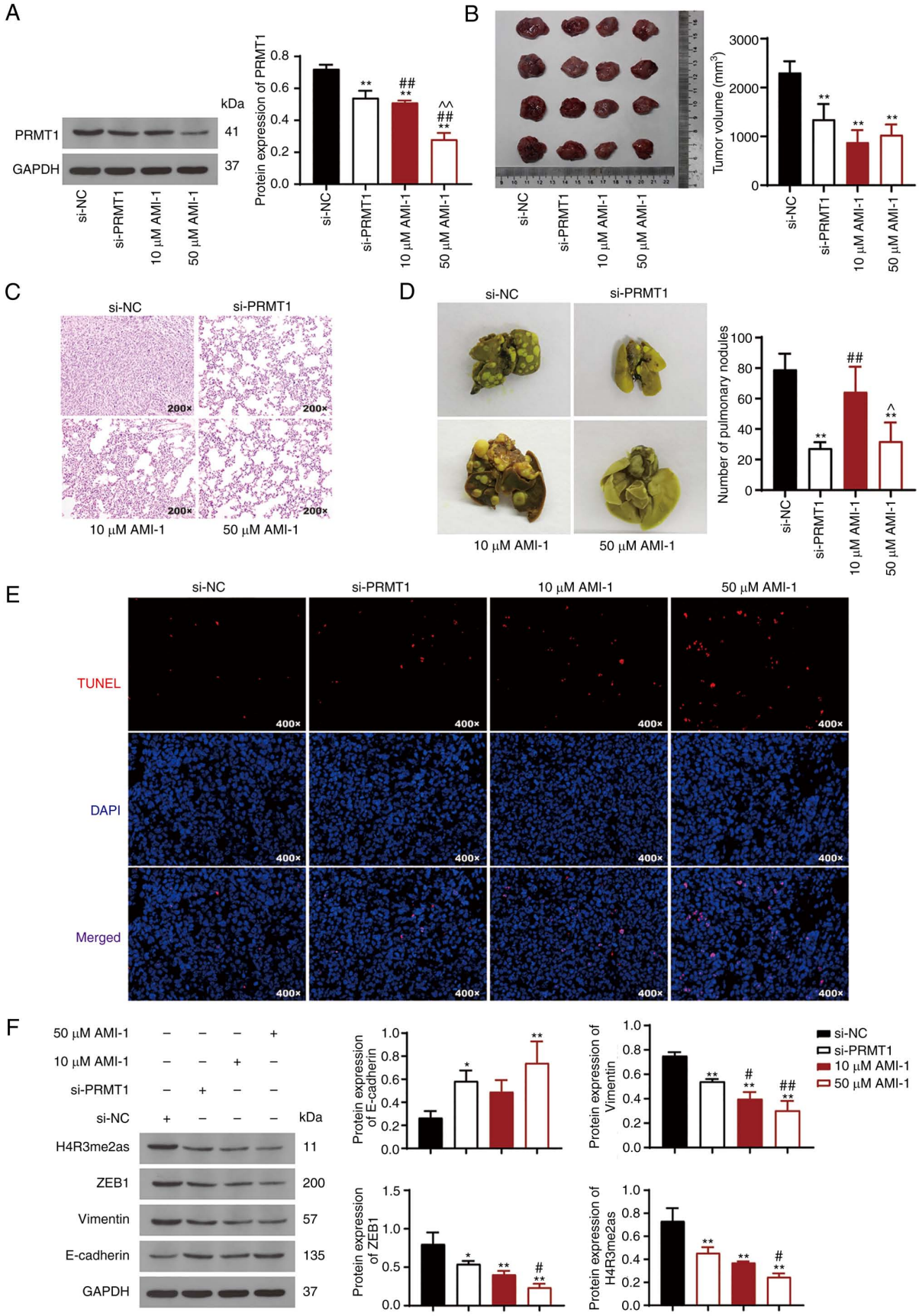

Figure 6. PRMT1 knockdown reduces tumor growth and metastasis by inhibiting ZEB1/H4R3me2as in a xenograft model. (A) PRMT1 protein expression in TC tissues (B) Excised tumors from the mouse model of TC. (C) H&E staining of TC tissues. Magnification, x200. (D) Image of pulmonary nodules and number of pulmonary nodules. (E) TUNEL assays were used to assess apoptosis in xenograft model mice. Magnification, x400. (F) Western blotting was to measure the protein expression levels of E-cadherin, vimentin, H4R3me2as, and ZEB1 in TC tissues. BALB/C nude mice were subcutaneously injected with treated 8505C cells. *P<0.05, **P<0.01 vs. si-NC; $^{\#}$P<0.05, $^{\#\#}$P<0.01 vs. si-PRMT1; $^{\wedge}$P<0.05; $^{\wedge\wedge}$P<0.01 vs. 10 μM AMI-1. PRMT1, protein arginine methyltransferase 1; ZEB1, zinc finger e-box binding homeobox1; H4R3me2as, asymmetric demethylation of H4 at the third arginine residue; TC, thyroid carcinoma; si-NC, small interfering RNA negative control.

therapy (31). EMT is orchestrated by a collection of transcription factors, including ZEB1, ZEB2, and zinc finger proteins (32). E-cadherin and vimentin are important mesenchymal biomarkers (33). E-cadherin is a tumor suppressor protein, and its downregulation in association with EMT frequently occurs during tumor metastasis (34). Vimentin is a filamentous protein that is confirmed to be upregulated during cancer metastasis (35). In the present study, E-cadherin expression was elevated, and vimentin expression was reduced following PRMT1 knockdown. Furthermore, the metastasis of TC cells to the lungs was observed, as evidenced by pulmonary nodule formation in mice. However, PRMT1 downregulation inhibited this pulmonary nodule formation. Collectively, these results revealed that PRMT1 participates in TC tumor progression and that its knockdown reduces metastasis.

H4R3me2as, a specific substrate of PRMT1, is a transcriptional activation marker (26). A previous study reported that the methylation of H4R3 by PRMT1 is necessary for the activation of its expression (36). PRMT1 regulates tumor-initiating properties through H4 arginine methylation in esophageal squamous cell carcinoma (37). The results of the present study revealed that H4R3me2as expression was regulated by PRMT1 and was related to TC progression. Previous studies demonstrated that PRMT1 participates in pancreatic cancer progression by targeting ZEB1 (21). ZEB1 is an EMT-related transcription factor (38). Abnormal ZEB1 expression has been confirmed in multiple types of cancer, including breast (39), colorectal (40), hepatocellular (41), and ovarian cancer (42). Morillo-Bernal *et al* (43) demonstrated that ZEB1 is a target of FOXE1 in regulating TC progression. In the present study, ZEB1 was upregulated in TC and tumor tissues. PRMT1 has been reported to function as an upstream mediator of the ZEB family of proteins (44). This upregulation also promotes EMT (45). These results also revealed that PRMT1 knockdown reduced ZEB1 expression in TC and tumor tissues. Based on these data, it is hypothesized that PRMT1 knockdown may suppress TC progression by downregulating ZEB1/H4R3me2as.

In conclusion, the present study showed that PRMT1 was upregulated in both TC and tumor-bearing mice. PRMT1 knockdown inhibited cell proliferation and migration and promoted apoptosis in TC. Importantly, it was shown that PRMT1 participated in TC progression by upregulating ZEB1 and H4R3me2as expression levels. These results provide critical insights into PRMT1-driven TC pathophysiology and treatment as well as identifying novel potential therapeutic targets and diagnostic biomarkers for the management of TC. However, further studies are required to confirm whether PRMT1 can influence the phenotypes of normal cells and uncover its clinical applicability. In addition, studies are required to verify the role of PRMT1 in the regulating of ZEB1 expression in TC progression.

Acknowledgements

Not applicable.

Funding

No funding was received.

Availability of data and materials

The datasets used and/or analyzed during the present study are available from the corresponding author on reasonable request.

Authors' contributions

GF conceived the study, collected the data, analyzed the data, and wrote and revised the manuscript. CC and YL designed the study and collected the data.

Ethics approval and consent to participate

All animal experiments were approved by the Institutional Animal Care and Use Committee of the Affiliated Hospital of the Zunyi Medical University (approval no. zyfy-an-2023-0185).

Patient consent for publication

Not applicable.

Competing interests

The authors declare that they have no competing interests.

References

1. Kleinschmidt-DeMasters B and Marshall C: Thyroid carcinoma metastases to central nervous system and vertebrae. Folia Neuropathol 60: 292-300, 2022.
2. Pan Z, Xu T, Bao L, Hu X, Jin T, Chen J, Chen J, Qian Y, Lu X, Li L, *et al*: CREB3L1 promotes tumor growth and metastasis of anaplastic thyroid carcinoma by remodeling the tumor microenvironment. Mol Cancer 21: 190, 2022.
3. Deng Y, Li X, Jiang W and Tang J: SNRPB promotes cell cycle progression in thyroid carcinoma via inhibiting p53. Open Med (Wars) 17: 1623-1631, 2022.
4. Franchini F, Palatucci G, Colao A, Ungaro P, Macchia PE and Nettore IC: Obesity and thyroid cancer risk: An update. Int J Environ Res Public Health 19: 1116, 2022.
5. Pan Y, Wu L, He S, Wu J, Wang T and Zang H: Identification of hub genes in thyroid carcinoma to predict prognosis by integrated bioinformatics analysis. Bioengineered 12: 2928-2940, 2021.
6. Sun R, Yang L, Wang Y, Zhang Y, Ke J and Zhao D: DNAJB11 predicts a poor prognosis and is associated with immune infiltration in thyroid carcinoma: A bioinformatics analysis. J Int Med Res 49: 3000605211053722, 2021.
7. Geng X, Sun Y, Fu J, Cao L and Li Y: MicroRNA-17-5p inhibits thyroid cancer progression by suppressing Early growth response 2 (EGR2). Bioengineered 12: 2713-2722, 2021.
8. Lv L, Wang X, Shen J, Cao Y and Zhang Q: MiR-574-3p inhibits glucose toxicity-induced pancreatic β-cell dysfunction by suppressing PRMT1. Diabetol Metab Syndr 14: 99, 2022.
9. Wang YC, Wang CW, Lin WC, Tsai YJ, Chang CP, Lee YJ, Lin MJ and Li C: Identification, chromosomal arrangements and expression analyses of the evolutionarily conserved prmt1 gene in chicken in comparison with its vertebrate paralogue prmt8. PLoS One 12: e0185042, 2017.
10. Yao B, Gui T, Zeng X, Deng Y, Wang Z, Wang Y, Yang D, Li Q, Xu P, Hu R, *et al*: PRMT1-mediated H4R3me2a recruits SMARCA4 to promote colorectal cancer progression by enhancing EGFR signaling. Genome Med 13: 58, 2021.
11. Kim E, Jang J, Park JG, Kim KH, Yoon K, Yoo BC and Cho JY: Protein Arginine methyltransferase 1 (PRMT1) selective inhibitor, TC-E 5003, has anti-inflammatory properties in TLR4 Signaling. Int J Mol Sci 21: 3058, 2020.
12. Matsubara H, Fukuda T, Awazu Y, Nanno S, Shimomura M, Inoue Y, Yamauchi M, Yasui T and Sumi T: PRMT1 expression predicts sensitivity to platinum-based chemotherapy in patients with ovarian serous carcinoma. Oncol Lett 21: 162, 2021.

13. Wang C, Dong L, Zhao Z, Zhang Z, Sun Y, Li C, Li G, You X, Yang X, Wang H and Hong W: Design and Synthesis of Novel PRMT1 inhibitors and investigation of their effects on the migration of cancer cell. Front Chem 10: 888727, 2022.
14. Gu X, He M, Lebedev T, Lin CH, Hua ZY, Zheng YG, Li ZJ, Yang JY and Li XG: PRMT1 is an important factor for medulloblastoma cell proliferation and survival. Biochem Biophys Rep 32: 101364, 2022.
15. Vezzalini M, Aletta JM, Beghelli S, Moratti E, Della Peruta M, Mafficini A, Mojica WD, Mombello A, Scarpa A and Sorio C: Immunohistochemical detection of arginine methylated proteins (MeRP) in archival tissues. Histopathology 57: 725-733, 2010.
16. Zhang Y, Liu X, Liang W, Dean DC, Zhang L and Liu Y: Expression and Function of ZEB1 in the Cornea. Cells 10: 925, 2021.
17. Wang X, Lai Q, He J, Li Q, Ding J, Lan Z, Gu C, Yan Q, Fang Y, Zhao X and Liu S: LncRNA SNHG6 promotes proliferation, invasion and migration in colorectal cancer cells by activating TGF-β/Smad signaling pathway via targeting UPF1 and inducing EMT via regulation of ZEB1. Int J Med Sci 16: 51-59, 2019.
18. Chen XJ, Deng YR, Wang ZC, Wei WF, Zhou CF, Zhang YM, Yan RM, Liang LJ, Zhong M, Liang L, *et al*: Hypoxia-induced ZEB1 promotes cervical cancer progression via CCL8-dependent tumour-associated macrophage recruitment. Cell Death Dis 10: 508, 2019.
19. Shen H, Zhu H, Chen Y, Shen Z, Qiu W, Qian C and Zhang J: ZEB1-induced LINC01559 expedites cell proliferation, migration and EMT process in gastric cancer through recruiting IGF2BP2 to stabilize ZEB1 expression. Cell Death Dis 12: 349, 2021.
20. Filipović J, Bosić M, Ćirović S, Životić M, Dunđerović D, Đorđević D, Živković-Perišić S, Lipkovski A and Marković-Lipkovski J: PRMT1 expression in renal cell tumors-application in differential diagnosis and prognostic relevance. Diagn Pathol 14: 120, 2019.
21. Lin Z, Chen Y, Lin Z, Chen C and Dong Y: Overexpressing PRMT1 inhibits proliferation and invasion in pancreatic cancer by inverse correlation of ZEB1. IUBMB Life 70: 1032-1039, 2018.
22. Livak KJ and Schmittgen TD: Analysis of relative gene expression data using real-time quantitative PCR and the 2(-Delta Delta C(T)) method. Methods 25: 402-408, 2001.
23. Saiselet M, Floor S, Tarabichi M, Dom G, Hébrant A, van Staveren WC and Maenhaut C: Thyroid cancer cell lines: An overview. Front Endocrinol (Lausanne) 3: 133, 2012.
24. Pozdeyev N, Berlinberg A, Zhou Q, Wuensch K, Shibata H, Wood WM and Haugen BR: Targeting the NF-κB pathway as a combination therapy for advanced thyroid cancer. PLoS One 10: e0134901, 2015.
25. Sung BY, Lin YH, Kong Q, Shah PD, Glick Bieler J, Palmer S, Weinhold KJ, Chang HR, Huang H, Avery RK, *et al*: Wnt activation promotes memory T cell polyfunctionality via epigenetic regulator PRMT1. J Clin Invest 132: e140508, 2022.
26. Thiebaut C, Eve L, Poulard C and Le Romancer M: Structure, activity, and function of PRMT1. Life (Basel) 11: 1147, 2021.
27. Yin XK, Wang YL, Wang F, Feng WX, Bai SM, Zhao WW, Feng LL, Wei MB, Qin CL, Wang F, *et al*: PRMT1 enhances oncogenic arginine methylation of NONO in colorectal cancer. Oncogene 40: 1375-1389, 2021.
28. Giuliani V, Miller MA, Liu CY, Hartono SR, Class CA, Bristow CA, Suzuki E, Sanz LA, Gao G, Gay JP, *et al*: PRMT1-dependent regulation of RNA metabolism and DNA damage response sustains pancreatic ductal adenocarcinoma. Nat Commun 12: 4626, 2021.
29. Shimomura M, Fukuda T, Awazu Y, Nanno S, Inoue Y, Matsubara H, Yamauchi M, Yasui T and Sumi T: PRMT1 expression predicts response to neoadjuvant chemotherapy for locally advanced uterine cervical cancer. Oncol Lett 21: 150, 2021.
30. Li Z, Wang D, Chen X, Wang W, Wang P, Hou P, Li M, Chu S, Qiao S, Zheng J and Bai J: PRMT1-mediated EZH2 methylation promotes breast cancer cell proliferation and tumorigenesis. Cell Death Dis 12: 1080, 2021.
31. Pastushenko I and Blanpain C: EMT transition states during tumor progression and metastasis. Trends Cell Biol 29: 212-226, 2019.
32. Pan G, Liu Y, Shang L, Zhou F and Yang S: EMT-associated microRNAs and their roles in cancer stemness and drug resistance. Cancer Commun (Lond) 41: 199-217, 2021.
33. Huang X, Xiang L, Wang B, Hu J, Liu C, Ren A, Du K, Ye G, Liang Y, Tang Y, *et al*: CMTM6 promotes migration, invasion, and EMT by interacting with and stabilizing vimentin in hepatocellular carcinoma cells. J Transl Med 19: 120, 2021.
34. Na TY, Schecterson L, Mendonsa AM and Gumbiner BM: The functional activity of E-cadherin controls tumor cell metastasis at multiple steps. Proc Natl Acad Sci USA 117: 5931-5937, 2020.
35. Usman S, Waseem NH, Nguyen TKN, Mohsin S, Jamal A, The MT and Waseem A: Vimentin is at the heart of epithelial mesenchymal transition (EMT) mediated metastasis. Cancers (Basel) 13: 4985, 2021.
36. Wagner S, Weber S, Kleinschmidt MA, Nagata K and Bauer UM: SET-mediated promoter hypoacetylation is a prerequisite for coactivation of the estrogen-responsive pS2 gene by PRMT1. J Biol Chem 281: 27242-27250, 2006.
37. Zhao Y, Lu Q, Li C, Wang X, Jiang L, Huang L, Wang C and Chen H: PRMT1 regulates the tumour-initiating properties of esophageal squamous cell carcinoma through histone H4 arginine methylation coupled with transcriptional activation. Cell Death Dis 10: 359, 2019.
38. Ramundo V, Zanirato G and Aldieri E: The epithelial-to-mesenchymal transition (EMT) in the development and metastasis of malignant pleural mesothelioma. Int J Mol Sci 22: 12216, 2021.
39. Wu HT, Zhong HT, Li GW, Shen JX, Ye QQ, Zhang ML and Liu J: Oncogenic functions of the EMT-related transcription factor ZEB1 in breast cancer. J Transl Med 18: 51, 2020.
40. Jin Z and Chen B: LncRNA ZEB1-AS1 regulates colorectal cancer cells by MiR-205/YAP1 Axis. Open Med (Wars) 15: 175-184, 2020.
41. Liu W, Zheng L, Zhang R, Hou P, Wang J, Wu L and Li J: Circ-ZEB1 promotes PIK3CA expression by silencing miR-199a-3p and affects the proliferation and apoptosis of hepatocellular carcinoma. Mol Cancer 21: 72, 2022.
42. Zhang J, Guan W, Xu X, Wang F, Li X and Xu G: A novel homeostatic loop of sorcin drives paclitaxel-resistance and malignant progression via Smad4/ZEB1/miR-142-5p in human ovarian cancer. Oncogene 40: 4906-4918, 2021.
43. Morillo-Bernal J, Fernández LP and Santisteban P: FOXE1 regulates migration and invasion in thyroid cancer cells and targets ZEB1. Endocr Relat Cancer 27: 137-151, 2020.
44. Soleymani L, Zarrabi A, Hashemi F, Hashemi F, Zabolian A, Banihashemi SM, Moghadam SS, Hushmandi K, Samarghandian S, Ashrafizadeh M and Khan H: Role of ZEB Family Members in Proliferation, Metastasis, and Chemoresistance of Prostate Cancer Cells: Revealing Signaling Networks. Curr Cancer Drug Targets 21: 749-767, 2021.
45. Iderzorig T, Kellen J, Osude C, Singh S, Woodman JA, Garcia C and Puri N: Comparison of EMT mediated tyrosine kinase inhibitor resistance in NSCLC. Biochem Biophys Res Commun 496: 770-777, 2018.